Malaya Journal of Matematik, Vol. 8, No. 4, 2215-2227, 2020

https://doi.org/10.26637/MJM0804/0153

Effects of uniform and non - uniform heat profiles on Darcy - Benard - Marangoni Convection in a composite layer comprising of couple stress fluid

R. Sumithra[1] and Shyamala Venkatraman[2]*

Abstract

The single component Darcy-Benard-Marangoni convection (DBMC) is investigated in a composite layer, comprising of an incompressible couple stress fluid. The upper boundary of the composite layer is free and the lower boundary is rigid. Both the boundaries of the composite layer are set under adiabatic condition. The eigen value problem is solved using exact technique considering the three heat profiles linear, Parabolic as well as inverted parabolic and respective expressions for Thermal Marangoni number (TMN) are obtained analytically for the Darcy model. The impact of various factors like couple stress parameters, thermal ratio, viscosity ratio, porous parameter and the horizontal wave number are graphically illustrated for all the three heat profiles.

Keywords

Marangoni convection, Couple Stress Fluid, Thermal Marangoni Number, Parabolic and Inverted Parabolic Heat Profiles.

AMS Subject Classification

76B07.

[1,2] *Department of UG, PG Studies & Research in Mathematics, Government Science College Autonomous, Bengaluru, Karnataka, India.*

***Corresponding author**: [2] svr02009@gmail.com

Article History: Received **24** September **2020**; Accepted **09** December **2020**

Contents

1 **Introduction** 2215
2 **Mathematical Formulation** 2216
3 **Boundary Conditions** 2217
4 **Solution by Exact Method** 2218
4.1 Linear Heat Profile 2219
4.2 Parabolic Heat Profile 2220
4.3 Inverted Parabolic Heat Profile 2221
5 **Interpretations** 2222
6 **Conclusion** 2226
References 2226

1. Introduction

Couple stress fluid flow is one among the major concepts over which research articles line up in the current scenario. Marangoni convection in a composite layer has inspired many researchers due to its applications in aircraft and automobile industries, oil flow in the reservoirs under the earth's surface, compound film growth etc. Research articles contributing to Marangoni convection in couple stress fluid flow are rarely available. Recently, **Sumithra and Shyamala [2020]** investigated the problem of Darcy-Benard Marangoni convection in a composite layer with free upper boundary and rigid lower boundary comprising of an incompressible couple stress fluid under adiabatic-adiabatic and isothermal-adiabatic conditions. **Anum et al [2020]** have examined the Marangoni boundary layer flow using single-wall and multi-wall carbon nanotubes over a Riga plate together with the phenomenon of radiation. **Asifa et al [2020]** have investigated the couple stress Nano fluid flow with convective heat transfer and viscous dissipation in the presence of magnetic field. **Gireesha and Sindhu [2020]** have studied the magneto hydro-dynamic flow of incompressible Casson fluid through an annular micro channel filled with porous material under natural convection along with heat generation/absorption. **Sumithra et al [2020]** have analyzed the effect of constant heat source/sink on single component Marangoni convection in a composite layer comprising of incompressible single component fluid saturated porous layer over which lies a layer of same fluid with constant heat source in both the layers. **Nur Zarifah Abdul Hameed et al**

[2019] have studied the onset of thermal convection in a binary fluid saturated an anisotropic porous medium under the effect of magnetic field and nonlinear temperature profile. **Rahamat Ellahi et al [2019]** investigated the effect of magnetic field on Couette-Poiseuille flow of couple stress fluid with temperature dependent viscosity. **Giovanni et al [2018]** have examined the bounds on heat transfer in Benard-Marangoni convection at infinite Prandtl number by means of upper bounds on the Nusselt number as a function of the Marangoni number. **Ilani & Ashmawy [2018]** have studied the incompressible couple stress fluid flow between two parallel plates with time dependent pressure gradient wherein one plate is kept stationary and the other one is in motion. **Sameena & Pranesh [2016]** have examined the effects of gravity modulations in an electrically conducting couple stress fluid with saturated porous layer. **Sanatan Das et al [2016]** have investigated the flow of the incompressible couple stress viscous fluid caused by a stretching sheet in the presence of thermal radiation. **Gupta & Kalta [2015]** have analyzed the effect of non-uniform temperature gradient on Marangoni convection in a layer of liquid which is relatively hotter or cooler. **Narasimha Murthy [2014]** has studied the mixed convection of couple stress fluid in a vertical channel under the influence of heat generation or heat absorption. **Shivakumara et al [2012]** have examined the effects of basic temperature gradients on the onset of convection in a layer of an incompressible couple stress fluid saturated porous medium. **Siti et al [2010]** have examined the effects of non-uniform temperature gradient along with magnetic field and constant heat flux on Benard-Marangoni convection. **Mahmud et al [2009]** have studied the effects of nonlinear temperature profile on Marangoni convective flow in micro polar fluid in the presence of magnetic field.

This research paper examines the effects of uniform and non-uniform heat profiles on single component DBMC in a composite layer comprising of couple stress fluid. The Thermal Marangoni number values versus depth ratio are tabulated for the linear, parabolic and inverted parabolic heat profiles. The impact of various factors like couple stress parameters, thermal ratio, viscosity ratio, porous parameter and the horizontal wave number are graphically illustrated for all the three heat profiles.

2. Mathematical Formulation

Let us consider an infinite horizontal layer of incompressible couple stress fluid of thickness **d** and underneath lies the porous layer saturated with same fluid, of thickness d_m in the vertical z-direction. The bottom surface of the porous layer is considered to be rigid and the upper surface of the fluid layer is free with surface tension effects depending on temperature and are maintained at different constant temperatures. A Cartesian coordinate system is considered with origin at the interface between porous and fluid layers and the z-axis, vertically upwards.

The basic equations for fluid and porous layer respectively governing such a system are,

$$\nabla \cdot \vec{q} = 0 \tag{2.1}$$

$$\rho_0[\frac{\partial \vec{q}}{\partial t} + (\vec{q} \cdot \nabla)\vec{q}] = -\nabla P + \mu \nabla^2 \vec{q} - \mu' \nabla^4 \vec{q} \tag{2.2}$$

$$\frac{\partial T}{\partial t} + (\vec{q} \cdot \nabla)T = \kappa \nabla^2 T \tag{2.3}$$

$$\nabla_m \cdot \vec{q_m} = 0 \tag{2.4}$$

$$\rho_0 \left[\frac{1}{\phi} \cdot \frac{\partial \vec{q_m}}{\partial t} + \frac{1}{\phi^2}(\vec{q_m} \cdot \nabla_m)\vec{q_m}\right] = -\nabla_m P_m - \frac{\mu}{K}\vec{q_m} + \frac{\mu_m'}{K}\nabla_m{}^2 \vec{q_m} \tag{2.5}$$

$$M\frac{\partial T_m}{\partial t} + (\vec{q_m} \cdot \nabla_m)T_m = \kappa_m \nabla_m{}^2 T_m \tag{2.6}$$

where $\vec{q} = (u, v, w)$ is the velocity vector, ρ_0 is the fluid density, t is the time, P is the pressure, μ is the fluid viscosity, μ' is the couple stress viscosity of the fluid in the fluid layer, T is the temperature, κ is the thermal diffusivity,ϕ is the porosity, K is the permeability, μ_m' is the couple stress viscosity of the fluid in the porous layer, M = $\frac{(\rho_0 C_p)_m}{(\rho_0 C_p)_f}$ is the ratio of heat capacities and the subscripts 'm' and'f' refer to respective quantities of the porous medium and the fluid respectively.

The basic state of the system being quiescent is described by

$$[u, v, w, P, T] = [0, 0, 0, P_b(z), T_b(z)] \tag{2.7}$$

in the fluid layer and

$$[u_m, v_m, w_m, P_m, T_m] = [0, 0, 0, P_{mb}(z_m), T_{mb}(z_m)] \tag{2.8}$$

in the porous layer where the subscript 'b' denotes the basic state.

The basic state temperature distributions $T_b(z)$ and $T_{mb}(z_m)$, respectively are found to be

$$T_b(z) = T_0 - \frac{(T_0 - T_U)g(z)}{d} \; in \; 0 \le z \le d \tag{2.9}$$

$$T_{mb}(z_m) = T_0 - \frac{(T_L - T_0)g_m(z_m)}{d_m} \; in \; 0 \le z_m \le d_m \tag{2.10}$$

where $T_0 = \dfrac{\kappa d_m T_u + \kappa_m d T_L}{\kappa_m d + \kappa d_m}$ is the interface temperature, g(z) and $g_m(z_m)$ are the nondimensional heat profiles.
In order to investigate the stability of the basic solution, infinitesimal disturbances are introduced in the form

$$[\overrightarrow{q}, P, T] = [0, P_b(z), T_b(z)] + [\overrightarrow{q}', P', \theta] \tag{2.11}$$

$$\& \ [\overrightarrow{q}_m, P_m, T_m] = [0, P_{mb}(z_m), T_{mb}(z_m)] + [\overrightarrow{q}'_m, P'_m, \theta_m] \tag{2.12}$$

where the primed ones are the perturbed ones over their equilibirium counterparts. Now (2.11) and (2.12) are substituted in to (2.1) to (2.6) and are linearized in the usual manner. Next, the pressure term is eliminated from (2.2) and (2.5) by taking curl twice on these two equations and only the vertical component is retained. The resulting equations are then non dimensionalised using $d, \dfrac{d^2}{\kappa}, \dfrac{\kappa}{d}, T_0 - T_U$ as the units of length, time, velocity and temperature in the fluid layer and $d_m, \dfrac{d_m^2}{\kappa_m}, \dfrac{\kappa_m}{d_m}, T_L - T_0$ as the corresponding characteristic quantities in the porous layer.

The dimensionless equations are then subjected to normal mode analysis as follows

$$\begin{bmatrix} W \\ \theta \end{bmatrix} = \begin{bmatrix} W(z) \\ \theta(z) \end{bmatrix} f(x,y) e^{nt} \tag{2.13}$$

and

$$\begin{bmatrix} W_m \\ \theta_m \end{bmatrix} = \begin{bmatrix} W_m(z_m) \\ \theta_m(z_m) \end{bmatrix} f(x_m, y_m) e^{n_m t} \tag{2.14}$$

with $\nabla^2 f + a^2 f = 0$ and $\nabla_m^2 f_m + a_m^2 f_m = 0$ where a and a_m are the nondimensional horizontal wave numbers, n and n_m are the frequencies, W and W_m are the dimensionless vertical velocities in fluid and porous layer respectively. Since the dimensional horizontal wave numbers must be the same for the fluid and porous layers, we must have $\dfrac{a}{d} = \dfrac{a_m}{d_m}$ and hence $a_m = \widehat{d}a$.
The following equations are obtained:
In $0 \le z \le 1$,

$$(D^2 - a^2)\left[(D^2 - a^2) - C_p(D^2 - a^2)^2 + \frac{n}{P_r}\right] W = 0 \tag{2.15}$$

$$[(D^2 - a^2) + n]\theta + W g(z) = 0 \tag{2.16}$$

In $-1 \le z_m \le 0$,

$$(D_m^2 - a_m^2)[C_{pm}(D_m^2 - a_m^2) + \frac{\beta^2}{P_{rm}} n_m - 1] W_m = 0 \tag{2.17}$$

$$[(D_m^2 - a_m^2) + M n_m]\theta_m + W_m g_m(z_m) = 0 \tag{2.18}$$

where, for the fluid layer, $C_p = \dfrac{\mu'}{\mu d^2}$ is the couple stress parameter, $Pr = \dfrac{\nu}{\kappa}$ is the Prandtl number, ν is the kinematic viscosity and for the porous layer, $C_{pm} = \dfrac{\mu'_m}{\mu {d_m}^2}$ is the couple stress parameter, $\beta^2 = \dfrac{K}{{d_m}^2} = Da$ is the Darcy number, β is the porous parameter, $Pr_m = \dfrac{\phi \nu}{\kappa_m}$ is the Prandtl number
Assuming that the present problem satisfies the principle of exchange of instability and hence putting $n = n_m = 0$, we get
In $0 \le z \le 1$,

$$(D^2 - a^2)^2[1 - C_p(D^2 - a^2)] W = 0 \tag{2.19}$$

$$(D^2 - a^2)\theta + W g(z) = 0 \tag{2.20}$$

In $-1 \le z_m \le 0$,

$$(D_m^2 - a_m^2)[1 - C_{pm}(D_m^2 - a_m^2)] W_m = 0 \tag{2.21}$$

$$(D_m^2 - a_m^2)\theta_m + W_m g_m(z_m) = 0 \tag{2.22}$$

3. Boundary Conditions

The suitable velocity and temperature boundary conditions are nondimensionalized and then subjected to normal mode expansion and are

$$\begin{aligned}
&W(1) = 0, \ \ D^3 W(1) - 3a^2 DW(1) = 0 \\
&\widehat{T} W(0) = W_m(0) \\
&\widehat{T}\widehat{d} DW(0) = \widehat{\mu} D_m W_m(0) \\
&\widehat{T}\widehat{d}^3 \beta^2 [D^3 W(0) - 3a^2 DW(0)] = \\
&- D_m W_m(0) + \widehat{\mu}\beta^2 [D_m^3 W_m(0) \\
&- 3a_m^2 D_m W_m(0)] W_m(-1) = 0 \\
&D_m^3 W_m(-1) - 3a_m^2 D_m W_m(-1) = 0 \\
&\widehat{T}\widehat{d}^2 (D^2 + a^2) W(0) = \widehat{\mu}(D_m^2 + a_m^2) W_m(0) \\
&D_m W_m(-1) = 0 \\
&D^2 W(1) + M_\theta \theta(1) a^2 = 0 \\
&D\theta(1) = 0 \\
&\theta(0) = \widehat{T}\theta_m(0) \\
&D\theta(0) = D_m \theta_m(0) \\
&D_m \theta_m(-1) = 0
\end{aligned} \tag{3.1}$$

where $M_\theta = -\frac{\partial \sigma_t}{\partial t}\frac{(T_0-T_U)d}{\mu\kappa}$ is the thermal Marangoni number. $\widehat{T} = \frac{T_L - T_0}{T_0 - T_U}$ is the thermal ratio. $\beta = \sqrt{\frac{K}{{d_m}^2}}$ is the porous parameter, $\widehat{d} = \frac{d_m}{d}$ is the depth ratio and $\widehat{\mu} = \frac{\mu_m}{\mu}$ where μ_m is the effective viscosity of the fluid in the porous layer.

4. Solution by Exact Method

The solutions W *and* W_m are obtained by solving (2.19) *and* (2.21) using the velocity boundary conditions of (3.1)

$$\begin{aligned} W(z) = A_1[&Cosh[az] + A_2 Sinh[az] + \\ &A_3 z Cosh[az] + A_4 z Sinh[az] + \\ &A_5 Cosh[\delta z] + A_6 Sinh[\delta z]] \end{aligned} \tag{4.1}$$

$$\begin{aligned} W_m(z) = A_1[&A_{m1} Cosh[a_m z_m] + A_{m2} Sinh[a_m z_m] + \\ &A_{m3} Cosh[\delta_m z_m] + A_{m4} Sinh[\delta_m z_m]] \end{aligned} \tag{4.2}$$

where $\delta = \sqrt{a^2 + \frac{1}{C_p}}$ and $\delta_m = \sqrt{a_m^2 + \frac{1}{C_{pm}}}$

where$A_i's : i = 2\ to\ 6$ *and* $A_{mj}'s : j = 1\ to\ 4$ are constants which are determined using the corresponding velocity boundary conditions as

$$\begin{aligned}
A_2 &= -\xi_{12}A_{m1} + \xi_{13}A_{m2} - \xi_{14}A_{m3} + \xi_{15}A_{m4} + \xi_{16} \\
A_3 &= \xi_7 A_{m1} + \xi_8 A_{m2} + \xi_9 A_{m3} + \xi_{10}A_{m4} - \xi_{11} \\
A_4 &= \xi_{17}A_{m1} + \xi_{18}A_{m3} + \xi_{19} \\
A_5 &= \frac{1}{\widehat{T}}(A_{m1} + A_{m3}) - 1 \\
A_6 &= \frac{-\xi_2}{\xi_1}A_{m1} - \frac{\xi_3}{\xi_1}A_{m2} - \frac{\xi_4}{\xi_1}A_{m3} - \frac{\xi_5}{\xi_1}A_{m4} + \frac{\xi_6}{\xi_1}
\end{aligned}$$

$$\begin{aligned} A_{m1} = \Bigg(&Tanh[a_m]\left(-\frac{I_1 I_4}{I_3} + I_2\right) + \frac{Cosh[\delta_m]}{Cosh[a_m]}\frac{I_4}{I_3} \\ &+ \frac{Sinh[\delta_m]}{Cosh[a_m]}\Bigg)A_{m4} \end{aligned}$$

$$\begin{aligned}
A_{m2} &= \left(-\frac{I_1 I_4}{I_3} + I_2\right)A_{m4} \\
A_{m3} &= \frac{-I_4}{I_3}A_{m4} \\
A_{m4} &= -\frac{\xi_{20}}{I_8} \\
\xi_1 &= Sinh[a]\frac{\delta^3 - 3a^2\delta}{2a^3} + Sinh[\delta] - Cosh[a]\frac{\delta^3 - a^2\delta}{2a^2}
\end{aligned}$$

$$\xi_2 = Sinh[a]\left(\frac{a_m^2\widehat{\mu}}{a\widehat{T}\widehat{d}^2} - \frac{\delta^2 + a^2}{2a\widehat{T}}\right) + \frac{Cosh[\delta]}{\widehat{T}}$$

$$\begin{aligned} \xi_3 = Sinh[a]&\left(\frac{a_m + 2a_m^3\widehat{\mu}\beta^2}{2a^3\widehat{T}\widehat{d}^3\beta^2}\right) + \\ &\frac{Cosh[a]}{\widehat{T}}\left(\widehat{\mu}a_m - \frac{a_m + 2a_m^3\widehat{\mu}\beta^2}{2a^2\widehat{d}^2\beta^2}\right) \end{aligned}$$

$$\begin{aligned}
\xi_4 &= Sinh[a]\left(\frac{\widehat{\mu}(\delta_m^2 + a_m^2)}{2a\widehat{T}\widehat{d}^2} - \frac{\delta^2 + a^2}{2a\widehat{T}}\right) + \frac{Cosh[\delta]}{\widehat{T}} \\
\xi_5 &= Sinh[a]\left(\frac{\delta_m - \widehat{\mu}\beta^2(\delta_m^3 - 3a_m^2\delta_m)}{2a^3\widehat{T}\widehat{d}^3\beta^2}\right) + \\
&\frac{Cosh[a]}{\widehat{T}\widehat{d}}\left(\widehat{\mu}\delta_m - \frac{\delta_m - \widehat{\mu}\beta^2(\delta_m^3 - 3a_m^2\delta_m)}{2a^2\widehat{d}^2\beta^2}\right) \\
\xi_6 &= -Sinh[a]\frac{\delta^2 - a^2}{2a} + Cosh[\delta] - Cosh[a] \\
\xi_7 &= \frac{\delta^3 - a^2\delta}{2a^2} \\
\xi_8 &= \frac{\delta^3 - a^2\delta}{2a^2}\frac{\xi_3}{\xi_1} + \frac{1}{\widehat{T}\widehat{d}}\left(\widehat{\mu}a_m - \frac{a_m + 2a_m^3\widehat{\mu}\beta^2}{2a^2\widehat{d}^2\beta^2}\right) \\
\xi_9 &= \frac{\delta^3 - a^2\delta}{2a^2}\frac{\xi_4}{\xi_1} \\
\xi_{10} &= \frac{\delta^3 - a^2\delta}{2a^2}\frac{\xi_5}{\xi_1} + \frac{1}{\widehat{T}\widehat{d}}\left(\widehat{\mu}\delta_m - \frac{\delta_m - \widehat{\mu}\beta^2(\delta_m^3 - 3a_m^2\delta_m)}{2a^2\widehat{d}^2\beta^2}\right) \\
\xi_{11} &= \frac{\delta^3 - a^2\delta}{2a^2}\frac{\xi_6}{\xi_1} \\
\xi_{12} &= \frac{\delta^3 - 3a^2\delta}{2a^3}\frac{\xi_2}{\xi_1} \\
\xi_{13} &= \frac{a_m + 2a_m^3\widehat{\mu}\beta^2}{2a^3\widehat{T}\widehat{d}^3\beta^2} - \frac{\delta^3 - 3a^2\delta}{2a^3}\frac{\xi_3}{\xi_1} \\
\xi_{14} &= \frac{\delta^3 - 3a^2\delta}{2a^3}\frac{\xi_4}{\xi_1} \\
\xi_{15} &= \frac{\delta_m - \widehat{\mu}\beta^2(\delta_m^3 - 3a_m^2\delta_m)}{2a^3\widehat{T}\widehat{d}^3\beta^2} - \frac{\delta^3 - 3a^2\delta}{2a^3}\frac{\xi_5}{\xi_1} \\
\xi_{16} &= \frac{\delta^3 - 3a^2\delta}{2a^3}\frac{\xi_6}{\xi_1} \\
\xi_{17} &= \frac{a_m^2\widehat{\mu}}{a\widehat{T}\widehat{d}^2} - \frac{\delta^2 + a^2}{2a\widehat{T}} \\
\xi_{18} &= \frac{\widehat{\mu}(\delta_m^2 + a_m^2)}{2a\widehat{T}} - \frac{\delta^2 + a^2}{2a\widehat{T}} \\
\xi_{19} &= \frac{\delta^2 - a^2}{2a} \\
\xi_{20} &= -2a^3 Sinh[a] - 2a^3 Cosh[a]\xi_{16} + 2a^3 Sinh[a]\xi_{11} - \\
&2a^3 Cosh[a]\xi_1 - (\delta^3 - 3a^2\delta)Sinh[\delta] + \\
&(\delta^3 - 3a^2\delta)Cosh[\delta]\frac{\xi_6}{\xi_1} \\
\xi_{21} &= 2a^3 Cosh[a]\xi_{12} - 2a^3 Sinh[a]\xi_7 - 2a^3 Cosh[a]\xi_{17} \\
&+ (\delta^3 - 3a^2\delta)Sinh[\delta]\frac{1}{\widehat{T}} - (\delta^3 - 3a^2\delta)Cosh[\delta]\frac{\xi_2}{\xi_1} \\
\xi_{22} &= -2a^3 Cosh[a]\xi_{13} - 2a^3 Sinh[a]\xi_8 -
\end{aligned}$$

$$(\delta^3-3a^2\delta)Cosh[\delta]\frac{\xi_3}{\xi_1}$$
$$\xi_{23}=2a^3Cosh[a]\xi_{14}-2a^3Sinh[a]\xi_9-2a^3Cosh[a]\xi_{18}$$
$$+(\delta^3-3a^2\delta)Sinh[\delta]\frac{1}{\widehat{T}}-(\delta^3-3a^2\delta)Cosh[\delta]\frac{\xi_4}{\xi_1}$$
$$\xi_{24}=-2a^3Cosh[a]\xi_{15}-2a^3Sinh[a]\xi_{10}-$$
$$(\delta^3-3a^2\delta)Cosh[\delta]\frac{\xi_5}{\xi_1}$$
$$I_1=-Sinh[a_m]Cosh[\delta_m]+\frac{\delta_m}{a_m}Cosh[a_m]Sinh[\delta_m]$$
$$I_2=Sinh[a_m]Sinh[\delta_m]-\frac{\delta_m}{a_m}Cosh[a_m]Cosh[\delta_m]$$
$$I_3=2a_m^3Sinh[a_m]Tanh[a_m]I_1-2a_m^3Tanh[a_m]Cosh[\delta_m]-$$
$$2a_m^3Cosh[a_m]I_1+(3a_m^2\delta_m-\delta_m^3)Sinh[\delta_m]$$

$$I_4=2a_m^3Sinh[a_m]Tanh[a_m]I_2+2a_m^3Tanh[a_m]Sinh[\delta_m]-$$
$$2a_m^3Cosh[a_m]I_2+(\delta_m^3-3a_m^2\delta_m)Cosh[\delta_m]$$

$$I_5=\xi_{21}\left(Tanh[a_m]\left(-\frac{I_1I_4}{I_3}+I_2\right)+\frac{Cosh[\delta_m]}{Cosh[a_m]}\frac{I_4}{I_3}+\frac{Sinh[\delta_m]}{Cosh[a_m]}\right)$$

$$I_6=\xi_{22}\left(-\frac{I_1I_4}{I_3}+I_2\right)$$
$$I_7=\frac{-I_4}{I_3}\xi_{23}$$
$$I_8=I_5+I_6+I_7+\xi_{24}$$

4.1 Linear Heat Profile

The profiles under consideration are

$$g(z)=1 \text{ and } g_m(z_m)=1 \tag{4.3}$$

Using (4.3) as well as the temperature boundary conditions from (3.1) in (2.20) & (2.22), the temperature distributions for Linear Profile are obtained as

$$\theta(z)=A_1\{D_1Cosh[az]+D_2Sinh[az]-f(z)\} \tag{4.4}$$

$$\theta_m(z)=A_1\{D_3Cosh[a_mz_m]+D_4Sinh[a_mz_m]-f_m(z_m)\} \tag{4.5}$$

where
$$f(z)=\frac{z}{2a}Sinh[az]+\frac{z}{2a}Cosh[az]A_2+$$
$$\left(\frac{z^2}{4a}Sinh[az]-\frac{z}{4a^2}Cosh[az]\right)A_3+$$
$$\left(\frac{z^2}{4a}Cosh[az]-\frac{z}{4a^2}Sinh[az]\right)A_4+$$
$$\frac{Cosh[\delta z]}{\delta^2-a^2}A_5+\frac{Sinh[\delta z]}{\delta^2-a^2}A_6$$
and
$$f_m(z_m)=\frac{z_m}{a_m}Sinh[a_mz_m]A_{m1}+\frac{z_m}{a_m}Cosh[a_mz_m]A_{m2}+$$
$$\frac{1}{\delta_m^2-a_m^2}Cosh[\delta_mz_m]A_{m3}+\frac{1}{\delta_m^2-a_m^2}Sinh[\delta_mz_m]A_{m4}$$
where,
$$\lambda_{59}=\frac{Cosh[a]}{2}+\frac{Sinh[a]}{2a}$$
$$\lambda_{60}=\frac{Sinh[a]}{2}+\frac{Cosh[a]}{2a}$$
$$\lambda_{61}=\frac{Cosh[a]}{4}+\frac{Sinh[a]}{4a}-\frac{Cosh[a]}{4a^2}$$
$$\lambda_{62}=\frac{Sinh[a]}{4}+\frac{Cosh[a]}{4a}-\frac{Sinh[a]}{4a^2}$$
$$\lambda_{63}=\frac{\delta Sinh[\delta]}{\delta^2-a^2}$$
$$\lambda_{64}=\frac{\delta Cosh[\delta]}{\delta^2-a^2}$$
$$\lambda_{65}=\lambda_{59}+A_2\lambda_{60}+A_3\lambda_{61}+A_4\lambda_{62}+A_5\lambda_{63}+A_6\lambda_{64}$$
$$\lambda_{66}=\frac{A_5}{\delta^2-a^2}-\frac{\widehat{T}A_{m3}}{\delta_m^2-a_m^2}$$
$$\lambda_{67}=\frac{A_2}{2a}-\frac{A_3}{4a^2}+\frac{A_6\,\delta}{\delta^2-a^2}$$
$$\lambda_{68}=\frac{A_{m2}}{a_m}+\frac{A_{m4}\,\delta_m}{\delta_m^2-a_m^2}$$
$$\lambda_{69}=\lambda_{67}-\lambda_{68}$$
$$\lambda_{70}=Cosh[a_m]+\frac{1}{a_m}Sinh[a_m]$$
$$\lambda_{71}=Sinh[a_m]+\frac{1}{a_m}Cosh[a_m]$$
$$\lambda_{72}=\frac{\delta_mSinh[\delta_m]}{\delta_m^2-a_m^2}$$
$$\lambda_{73}=\frac{\delta_mCosh[\delta_m]}{\delta_m^2-a_m^2}$$
$$\lambda_{74}=A_{m1}\lambda_{70}-A_{m2}\lambda_{71}+A_{m3}\lambda_{72}-A_{m4}\lambda_{73}$$

From the boundary conditions (3.1), we have the thermal Marangoni number

$$M_\theta=\frac{-D^2W(1)}{a^2\theta(1)}$$

The TMN for Linear Heat Profile which is $M_{\theta1}$ is obtained as
$$M_{\theta1}=\frac{-1}{a^2}\left(\frac{B_1}{B_2}\right)$$
where,
$$B_1=a^2Cosh[a]+a^2Sinh[a]A_2+J_1A_3+J_2A_4+$$
$$\delta^2Cosh[\delta]A_5+\delta^2Sinh[\delta]A_6$$
$$B_2=D_1Cosh[a]+D_2Sinh[a]-\frac{1}{2a}Sinh[a]-$$
$$\frac{1}{2a}Cosh[a]A_2-J_3A_3-J_4A_4-J_5A_5-J_6A_6$$

where,
$$J_1=2aSinh[a]+a^2Cosh[a]$$

$$J_2 = 2aCosh[a] + a^2 Sinh[a]$$

$$J_3 = \frac{1}{4a} Sinh[a] - \frac{1}{4a^2} Cosh[a]$$

$$J_4 = \frac{1}{4a} Cosh[a] - \frac{1}{4a^2} Sinh[a]$$

$$J_5 = \frac{Cosh[\delta]}{\delta^2 - a^2}$$

$$J_6 = \frac{Sinh[\delta]}{\delta^2 - a^2}$$

4.2 Parabolic Heat Profile

The profiles under consideration are

$$g(z) = 2z \text{ and } g_m(z_m) = 2z_m \tag{4.6}$$

Using (4.6) as well as the temperature boundary conditions from (3.1) in (2.20) & (2.22), the temperature distributions for Parabolic Profile are obtained as

$$\theta(z) = A_1\{D_1 Cosh[az] + D_2 Sinh[az] - f(z)\} \tag{4.7}$$

$$\theta_m(z) = A_1\{D_3 Cosh[a_m z_m] + D_4 Sinh[a_m z_m] - f_m(z_m)\} \tag{4.8}$$

where

$$f(z) = \left(\frac{z^2}{2a} Sinh[az] - \frac{z}{2a^2} Cosh[az]\right) +$$
$$A_2\left(\frac{z^2}{2a} Cosh[az] - \frac{z}{2a^2} Sinh[az]\right) +$$
$$A_3\left(\frac{z^3}{3a} Sinh[az] - \frac{z^2}{2a^2} Cosh[az] + \frac{z}{2a^3} Sinh[az]\right) +$$
$$A_4\left(\frac{z^3}{3a} Cosh[az] - \frac{z^2}{2a^2} Sinh[az] + \frac{z}{2a^3} Cosh[az]\right) +$$
$$A_5\left(\frac{2z Cosh[\delta z]}{\delta^2 - a^2} - \frac{4\delta Sinh[\delta z]}{(\delta^2 - a^2)^2}\right) +$$
$$A_6\left(\frac{2z Sinh[\delta z]}{\delta^2 - a^2} - \frac{4\delta Cosh[\delta z]}{(\delta^2 - a^2)^2}\right)$$

and

$$f_m(z_m) = \left(\frac{{z_m}^2}{2a_m} Sinh[a_m z_m] - \frac{z_m}{2{a_m}^2} Cosh[a_m z_m]\right) A_{m1} +$$
$$\left(\frac{{z_m}^2}{2a_m} Cosh[a_m z_m] - \frac{z_m}{2{a_m}^2} Sinh[a_m z_m]\right) A_{m2} +$$
$$\left(\frac{2z_m Cosh[\delta_m z_m]}{{\delta_m}^2 - {a_m}^2} - \frac{4\delta_m Sinh[\delta_m z_m]}{({\delta_m}^2 - {a_m}^2)^2}\right) A_{m3} +$$
$$\left(\frac{2z_m Sinh[\delta_m z_m]}{{\delta_m}^2 - {a_m}^2} - \frac{4\delta_m Cosh[\delta_m z_m]}{({\delta_m}^2 - {a_m}^2)^2}\right) A_{m4}$$

where,

$$\lambda_{59} = \frac{Cosh[a]}{2} + \frac{Sinh[a]}{2a} - \frac{Cosh[a]}{2a^2}$$

$$\lambda_{60} = \frac{Sinh[a]}{2} + \frac{Cosh[a]}{2a} - \frac{Sinh[a]}{2a^2}$$

$$\lambda_{61} = \frac{Cosh[a]}{3} + \frac{Sinh[a]}{2a} - \frac{Cosh[a]}{2a^2} + \frac{Sinh[a]}{2a^3}$$

$$\lambda_{62} = \frac{Sinh[a]}{3} + \frac{Cosh[a]}{2a} - \frac{Sinh[a]}{2a^2} + \frac{Cosh[a]}{2a^3}$$

$$\lambda_{63} = \frac{2\delta Sinh[\delta]}{\delta^2 - a^2} - \frac{2(a^2 + \delta^2) Cosh[\delta]}{(\delta^2 - a^2)^2}$$

$$\lambda_{64} = \frac{2\delta Cosh[\delta]}{\delta^2 - a^2} - \frac{2(a^2 + \delta^2) Sinh[\delta]}{(\delta^2 - a^2)^2}$$

$$\lambda_{65} = \lambda_{59} + A_2\lambda_{60} + A_3\lambda_{61} + A_4\lambda_{62} + A_5\lambda_{63} + A_6\lambda_{64}$$

$$\lambda_{66} = \frac{4\widehat{T}\delta_m A_{m4}}{(\delta_m^2 - a_m^2)^2} - \frac{4\delta A_6}{(\delta^2 - a^2)^2}$$

$$\lambda_{67} = \frac{-1}{2a^2} + \frac{A_4}{2a^3} - \frac{2(a^2 + \delta^2) A_5}{(\delta^2 - a^2)^2}$$

$$\lambda_{68} = \frac{-A_{m1}}{2{a_m}^2} - \frac{2({a_m}^2 + {\delta_m}^2) A_{m3}}{({\delta_m}^2 - {a_m}^2)^2}$$

$$\lambda_{69} = \lambda_{67} - \lambda_{68}$$

$$\lambda_{70} = \frac{Cosh[a_m]}{2} + \frac{Sinh[a_m]}{2a_m} - \frac{Cosh[a_m]}{2{a_m}^2}$$

$$\lambda_{71} = \frac{-Sinh[a_m]}{2} - \frac{Cosh[a_m]}{2a_m} + \frac{Sinh[a_m]}{2{a_m}^2}$$

$$\lambda_{72} = \frac{2\delta_m Sinh[\delta_m]}{\delta_m^2 - a_m^2} - \frac{2({a_m}^2 + {\delta_m}^2) Cosh[\delta_m]}{({\delta_m}^2 - {a_m}^2)^2}$$

$$\lambda_{73} = \frac{-2\delta_m Cosh[\delta_m]}{\delta_m^2 - a_m^2} - \frac{2({a_m}^2 + {\delta_m}^2) Sinh[\delta_m]}{({\delta_m}^2 - {a_m}^2)^2}$$

$$\lambda_{74} = A_{m1}\lambda_{70} + A_{m2}\lambda_{71} + A_{m3}\lambda_{72} + A_{m4}\lambda_{73}$$

From the boundary conditions (3.1), we have the thermal Marangoni number

$$M_\theta = \frac{-D^2 W(1)}{a^2 \theta(1)}$$

The TMN for Linear Heat Profile which is $M_{\theta 2}$ is obtained as

$$M_{\theta 2} = \frac{-1}{a^2}\left(\frac{B_1}{B_2}\right)$$

where,

$$B_1 = a^2 Cosh[a] + a^2 Sinh[a] A_2 + J_1 A_3 + J_2 A_4 +$$
$$\delta^2 Cosh[\delta] A_5 + \delta^2 Sinh[\delta] A_6$$

$$B_2 = D_1 Cosh[a] + D_2 Sinh[a] - \frac{1}{2a} Sinh[a] -$$
$$\frac{1}{2a} Cosh[a] A_2 - J_3 A_3 - J_4 A_4 - J_5 A_5 - J_6 A_6$$

where,

$$J_1 = 2aSinh[a] + a^2 Cosh[a]$$

$$J_2 = 2aCosh[a] + a^2 Sinh[a]$$

$$J_3 = \frac{1}{4a} Sinh[a] - \frac{1}{4a^2} Cosh[a]$$

$$J_4 = \frac{1}{4a} Cosh[a] - \frac{1}{4a^2} Sinh[a]$$

$$J_5 = \frac{Cosh[\delta]}{\delta^2 - a^2}$$
$$J_6 = \frac{Sinh[\delta]}{\delta^2 - a^2}$$

4.3 Inverted Parabolic Heat Profile

The profiles under consideration are

$$g(z) = 2(1-z) \text{ and } g_m(z_m) = 2(1-z_m) \tag{4.9}$$

Using (4.9) as well as the temperature boundary conditions from (3.1) in (2.20) & (2.22), the temperature distributions for Inverted Parabolic Profile are obtained as

$$\theta(z) = A_1\{D_1 Cosh[az] + D_2 Sinh[az] - f(z)\} \tag{4.10}$$

$$\theta_m(z) = A_1\{D_3 Cosh[a_m z_m] + D_4 Sinh[a_m z_m] - f_m(z_m)\} \tag{4.11}$$

where

$$f(z) = \left(\frac{z}{a}Sinh[az] - \frac{z^2}{2a}Sinh[az] + \frac{z}{2a^2}Cosh[az]\right) + A_2\left(\frac{z}{a}Cosh[az] - \frac{z^2}{2a}Cosh[az] + \frac{z}{2a^2}Sinh[az]\right) + A_3\left(\frac{z^2}{2a}Sinh[az] - \frac{z}{2a^2}Cosh[az] - \frac{z^3}{3a}Sinh[az] + \frac{z^2}{2a^2}Cosh[az] - \frac{z}{2a^3}Sinh[az]\right) + A_4\left(\frac{z^2}{2a}Cosh[az] - \frac{z}{2a^2}Sinh[az] - \frac{z^3}{3a}Cosh[az] + \frac{z^2}{2a^2}Sinh[az] - \frac{z}{2a^3}Cosh[az]\right) + A_5\left(\frac{2Cosh[\delta z]}{\delta^2 - a^2} - \frac{2zCosh[\delta z]}{\delta^2 - a^2} + \frac{4\delta Sinh[\delta z]}{(\delta^2 - a^2)^2}\right) + A_6\left(\frac{2Sinh[\delta z]}{\delta^2 - a^2} - \frac{2zSinh[\delta z]}{\delta^2 - a^2} + \frac{4\delta Cosh[\delta z]}{(\delta^2 - a^2)^2}\right)$$

and

$$f_m(z_m) = \left(\frac{z_m}{a_m}Sinh[a_m z_m] - \frac{{z_m}^2}{2a_m}Sinh[a_m z_m] + \frac{z_m}{2{a_m}^2}Cosh[a_m z_m]\right)A_{m1} + \left(\frac{z_m}{a_m}Cosh[a_m z_m] - \frac{{z_m}^2}{2a_m}Cosh[a_m z_m] + \frac{z_m}{2{a_m}^2}Sinh[a_m z_m]\right)A_{m2} + \left(\frac{2Cosh[\delta_m z_m]}{{\delta_m}^2 - {a_m}^2} - \frac{2z_m Cosh[\delta_m z_m]}{{\delta_m}^2 - {a_m}^2} + \frac{4\delta_m Sinh[\delta_m z_m]}{({\delta_m}^2 - {a_m}^2)^2}\right)A_{m3} + \left(\frac{2Sinh[\delta_m z_m]}{{\delta_m}^2 - {a_m}^2} - \frac{2z_m Sinh[\delta_m z_m]}{{\delta_m}^2 - {a_m}^2} + \frac{4\delta_m Cosh[\delta_m z_m]}{({\delta_m}^2 - {a_m}^2)^2}\right)A_{m4}$$

where,

$$\lambda_{59} = \frac{Cosh[a]}{2} + \frac{Sinh[a]}{2a} + \frac{Cosh[a]}{2a^2}$$
$$\lambda_{60} = \frac{Sinh[a]}{2} + \frac{Cosh[a]}{2a} + \frac{Sinh[a]}{2a^2}$$
$$\lambda_{61} = \frac{Cosh[a]}{6} - \frac{Sinh[a]}{2a^3}$$
$$\lambda_{62} = \frac{Sinh[a]}{6} - \frac{Cosh[a]}{2a^3}$$
$$\lambda_{63} = \frac{-2Cosh[\delta]}{\delta^2 - a^2} + \frac{4\delta^2 Cosh[\delta]}{(\delta^2 - a^2)^2}$$
$$\lambda_{64} = \frac{-2Sinh[\delta]}{\delta^2 - a^2} + \frac{4\delta^2 Sinh[\delta]}{(\delta^2 - a^2)^2}$$
$$\lambda_{65} = \lambda_{59} + A_2\lambda_{60} + A_3\lambda_{61} + A_4\lambda_{62} + A_5\lambda_{63} + A_6\lambda_{64}$$
$$\lambda_{66} = \frac{2\widehat{T}A_{m3}}{\delta_m^2 - a_m^2} + \frac{4\widehat{T}\delta_m A_{m4}}{(\delta_m^2 - a_m^2)^2} - \frac{2A_5}{\delta^2 - a^2} - \frac{4\delta A_6}{(\delta^2 - a^2)^2}$$
$$\lambda_{67} = \frac{1}{2a^2} + \frac{A_2}{a} - \frac{A_3}{2a^2} - \frac{A_4}{2a^3} + \left(\frac{-2}{\delta^2 - a^2} + \frac{4\delta^2}{(\delta^2 - a^2)^2}\right)A_5 + \frac{2\delta}{\delta^2 - a^2}A_6$$
$$\lambda_{68} = \frac{A_{m1}}{2{a_m}^2} + \frac{A_{m2}}{a_m} + \left(\frac{-2}{{\delta_m}^2 - {a_m}^2} + \frac{4{\delta_m}^2}{({\delta_m}^2 - {a_m}^2)^2}\right)A_{m3} + \frac{2\delta_m}{{\delta_m}^2 - {a_m}^2}A_{m4}$$
$$\lambda_{69} = \lambda_{67} - \lambda_{68}$$
$$\lambda_{70} = \frac{3Cosh[a_m]}{2} + \frac{Sinh[a_m]}{2a_m} - \frac{Cosh[a_m]}{2{a_m}^2}$$
$$\lambda_{71} = \frac{3Sinh[a_m]}{2} + \frac{Cosh[a_m]}{2a_m} - \frac{Sinh[a_m]}{2{a_m}^2}$$

$$\lambda_{72} = \frac{4\delta_m Sinh[\delta_m]}{\delta_m^2 - a_m^2} + \frac{2Cosh[\delta_m]}{{\delta_m}^2 - {a_m}^2} - \frac{4{\delta_m}^2 Cosh[\delta_m]}{({\delta_m}^2 - {a_m}^2)^2}$$

$$\lambda_{73} = \frac{4\delta_m Cosh[\delta_m]}{\delta_m^2 - a_m^2} + \frac{2Sinh[\delta_m]}{{\delta_m}^2 - {a_m}^2} - \frac{4{\delta_m}^2 Sinh[\delta_m]}{({\delta_m}^2 - {a_m}^2)^2}$$

$$\lambda_{74} = A_{m1}\lambda_{70} - A_{m2}\lambda_{71} + A_{m3}\lambda_{72} - A_{m4}\lambda_{73}$$

From the boundary conditions (3.1), we have the thermal Marangoni number

$$M_\theta = \frac{-D^2 W(1)}{a^2 \theta(1)}$$

The TMN for Inverted Parabolic Heat Profile which is $M_{\theta 3}$ is obtained as

$$M_{\theta 3} = \frac{-1}{a^2}\left(\frac{B_1}{B_2}\right)$$

where,

$$B_1 = a^2 Cosh[a] + a^2 Sinh[a]A_2 + J_1 A_3 + J_2 A_4 + \delta^2 Cosh[\delta]A_5 + \delta^2 Sinh[\delta]A_6$$

$$B_2 = D_1 Cosh[a] + D_2 Sinh[a] - \frac{1}{2a}Sinh[a] - \frac{1}{2a}Cosh[a]A_2 - J_3 A_3 - J_4 A_4 - J_5 A_5 - J_6 A_6$$

where,

$$J_1 = 2aSinh[a] + a^2 Cosh[a]$$

$$J_2 = 2aCosh[a] + a^2 Sinh[a]$$

$$J_3 = \frac{1}{4a}Sinh[a] - \frac{1}{4a^2}Cosh[a]$$

$$J_4 = \frac{1}{4a}Cosh[a] - \frac{1}{4a^2}Sinh[a]$$

$$J_5 = \frac{Cosh[\delta]}{\delta^2 - a^2}$$

$$J_6 = \frac{Sinh[\delta]}{\delta^2 - a^2}$$

The terms common in the three cases are as follows:

$$D_1 = \frac{\lambda_{79}}{\lambda_{80}}$$

$$D_2 = \frac{\lambda_{78}}{\lambda_{77}}$$

$$D_3 = \widehat{T} D_1 - \lambda_{66}$$

$$D_4 = \frac{a}{a_m} D_2 - \frac{\lambda_{69}}{a_m}$$

$$\lambda_{75} = \frac{-1}{\widehat{T}} a_m Sinh[a_m]$$

$$\lambda_{76} = Cosh[a_m]\lambda_{69} - \frac{1}{\widehat{T}} a_m Sinh[a_m]\lambda_{66} - \lambda_{74}$$

$$\lambda_{77} = aCosh[a]\lambda_{75} - a^2 Sinh[a]Cosh[a_m]$$

$$\lambda_{78} = \lambda_{65}\lambda_{75} - \lambda_{76}(aSinh[a])$$

$$\lambda_{79} = \lambda_{77}\lambda_{76} - aCosh[a_m]\lambda_{78}$$

$$\lambda_{80} = \lambda_{77}\lambda_{75}$$

5. Interpretations

The three TMNs $M_{\theta 1}$, $M_{\theta 2}$ and $M_{\theta 3}$ for the linear, parabolic and inverted parabolic heat profiles respectively are obtained in terms of parameters such as horizontal wave numbers 'a' for the fluid & $'a'_m$ for porous layer, porous parameter $'\beta'$, thermal ratio $'\widehat{T}'$, viscosity ratio $'\widehat{\mu}'$, couple stress parameters $'C'_p$ & $'C'_{pm}$ for fluid and porous layers. The thermal Marangoni number M_θ versus depth ratio $'\widehat{d}'$ is shown graphically for the three profiles. The effects of the variations of each of these parameters on thermal Marangoni number with all other parameters unaltered is displayed in figures 2,3,4,5,6 and 7.The pattern of the curves for parabolic and inverted parabolic profiles are same but that of linear profile is different. That is, for linear profile, when the value of depth ratio increases, the thermal Marangoni number increases, but for parabolic and inverted parabolic profiles, as the value of depth ratio increases, the thermal Marangoni number is found to decrease. A comparison of values of thermal Marangoni number M_θ against depth ratio $'\widehat{d}'$ while fixing the values of other parameters as a=1,$C_p = 0.3$,$C_{pm} = 0.7$,$\beta = 0.1$, $\widehat{T} = 0.7$ & $\widehat{\mu} = 1$ is shown for the three profiles in table 1. From these values it is clear that the thermal Marangoni number for linear profile is higher indicating that this profile is the most stabilising one whereas the inverted parabolic profile is the most unstable one.

$\widehat{d}$	M_θ		
	Linear Profile	Parabolic Profile	Inverted Parabolic Profile
4.0	49.3891	2.36992	0.383055
4.4	50.3807	1.49919	0.343668
4.8	51.1637	1.05251	0.309491
5.2	51.7950	0.788913	0.279604
5.6	52.3128	0.61835	0.253354
6.0	52.7439	0.500588	0.23023
6.4	53.1073	0.415285	0.209808
6.8	53.4172	0.351173	0.191729
7.2	53.6840	0.301567	0.175686
7.6	53.9158	0.262255	0.16141
8.0	54.1186	0.230508	0.148683

Table1: Comparison of Thermal Marangoni Number for Linear, Parabolic and Inverted Parabolic Heat Profiles

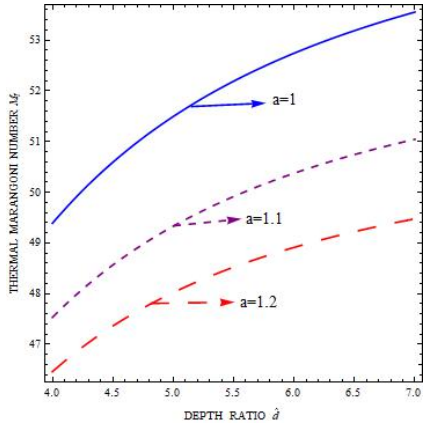

(a)

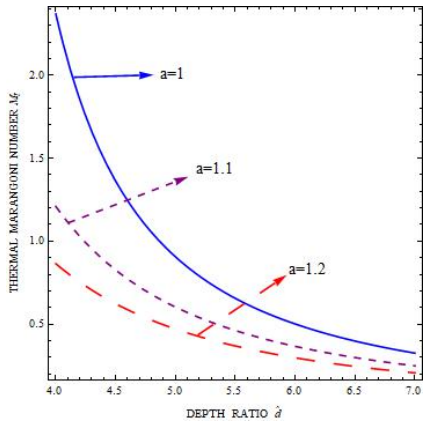

(b)

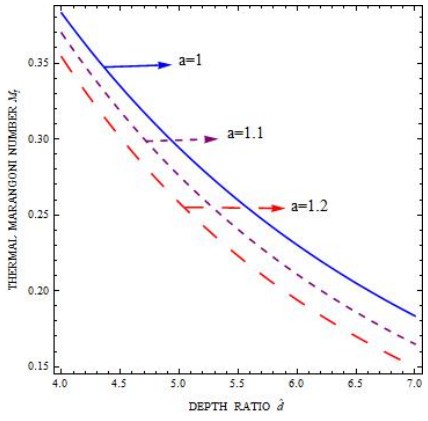

(c)

Figure2: Effects of horizontal wave number 'a'

The effects of 'a', the horizontal wave number for the fluid layer on the thermal Marangoni number are shown in figure 2a, 2b & 2c for linear, parabolic and inverted parabolic profiles respectively for the assigned values a=1, 1.1, 1.2. In parabolic profile the curves are converging whereas slight divergence is noticed in case of linear and inverted parabolic profiles. Similar effect of horizontal wave number is observed in all the three profiles i.e., increase in horizontal wave number decreases the Marangoni number, hence the increase in horizontal wave number destabilizes the system.

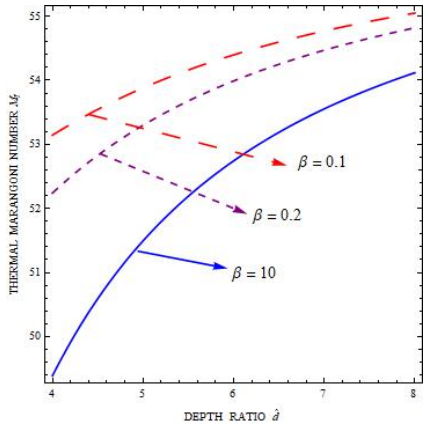

(a)

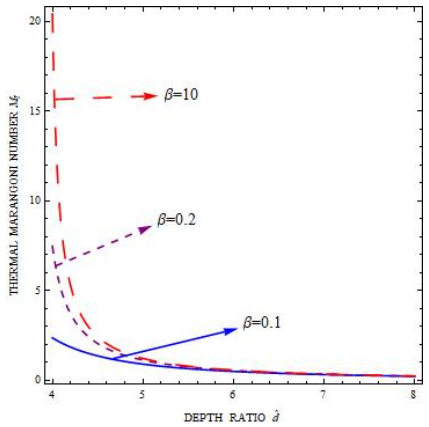

(b)

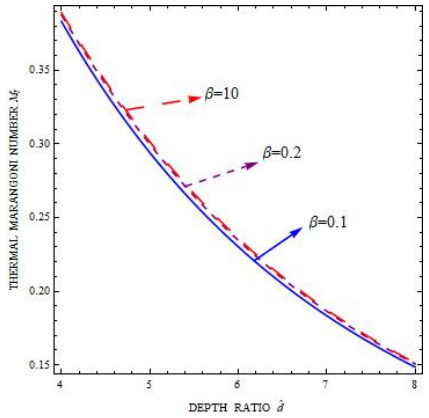

(c)

Figure3: Effects of porous parameter 'β'

The effects of porous parameter $'\beta'$ on the thermal Marangoni number are shown in figures 3a, 3b & 3c for linear, parabolic and inverted parabolic profiles respectively for β = 0.1, 0.2

and 10. The curves are converging in linear and parabolic profiles. It is observed that in linear and parabolic profile the variation effect of porous parameter is prominent for the composite layer with $d >> d_m$. Slight variation is found for inverted parabolic profile through all depth ratios. The increase in porous parameter increases the Marangoni number in case of all the three profiles. That is, the increase in permeability of the porous layer or the more space for the fluid to move is making the system stable which is quite unexpected, may be due to the nature of couple stress fluid.

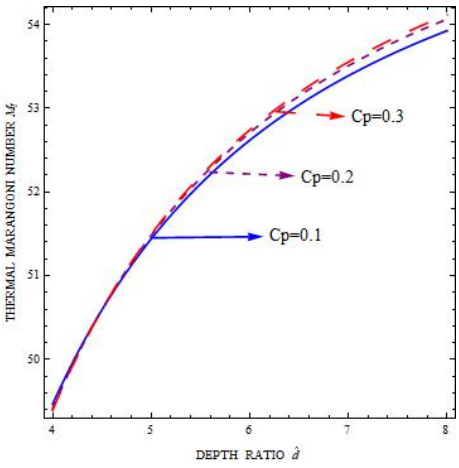

(a)

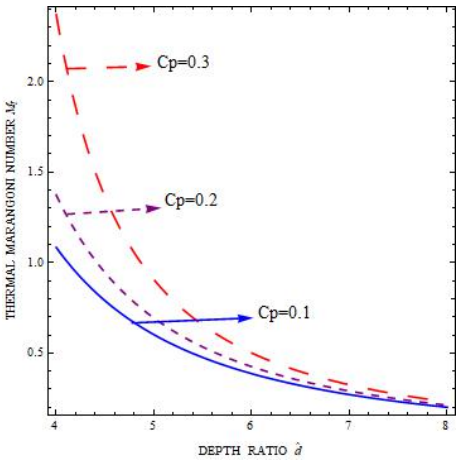

(b)

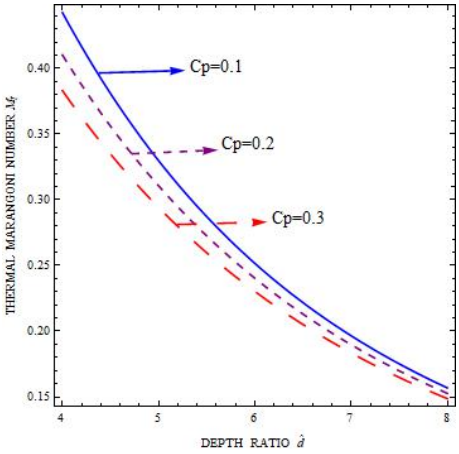

(c)

Figure4: Effects of couple stress parameter in the fluid layer'C_p'

The effects of couple stress parameter in the fluid layer $'C_p'$ on the thermal Marangoni number are shown in figure 4a, 4b & 4c for the values of C_p = 0.1, 0.2, 0.3. Here, similar effect is observed between linear and parabolic profiles i.e., the Marangoni mumber increases with increase in C_p whereas the effect of C_p is reversed in case of inverted parabolic profile. The curves are found diverging in case of linear profile and converging for both parabolic and inverted parabolic profiles. The couple stress parameter is prominent in porous layer dominant composite layer in the case of linear profile whereas the same is prominent in the fluid layer dominant composite layer in the parabolic and inverted parabolic profiles.

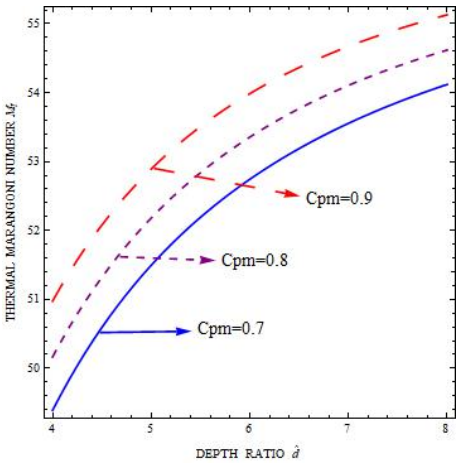

(a)

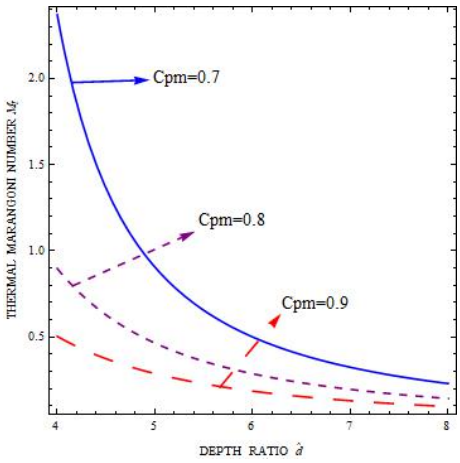

(b)

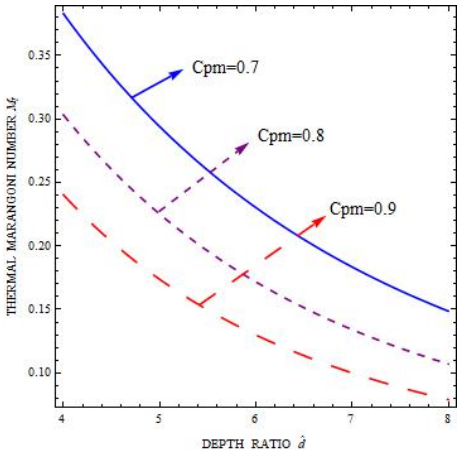

(c)

Figure5: Effects of couple stress parameter in the porous layer'C_{pm}'

The effects of couple stress parameter in the porous layer $'C'_{pm}$ on the thermal Marangoni number are shown in figure 5a, 5b & 5c for linear, parabolic and inverted parabolic profiles respectively for C_{pm} = 0.7, 0.8 and 0.9. The curves are found converging for parabolic profile. Very less convergence is noticed in case of linear and inverted parabolic profiles. The increase in the value of Couple stress parameter in the porous layer increases the thermal Marangoni number for the linear profile and the effect of the same decreases the thermal Marangoni number for the parabolic and inverted parabolic profiles.

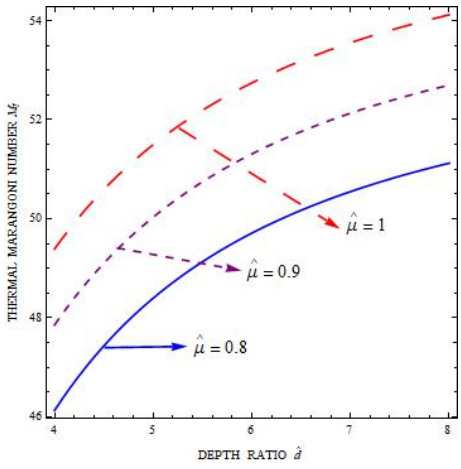

(a)

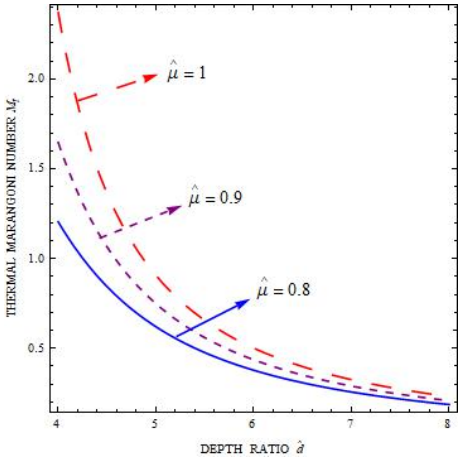

(b)

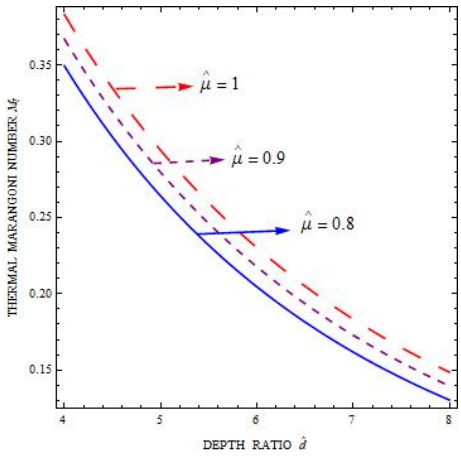

(c)

Figure6: Effects of viscosity ratio'$\widehat{\mu}$'

The effects of viscosity ratio $'\widehat{\mu}'$ on the thermal Marangoni number are shown in figure 6a, 6b and 6c for linear, parabolic & inverted parabolic profiles respectively for the values of $\widehat{\mu}$ =

0.8, 0.9 and 1. Variation effect of $\widehat{\mu}$ found unaltered for all the values of depth ratios for linear and inverted parabolic profiles and the curves are diverging in case of parabolic profile. It is evident that thermal Marangoni number increases when $\widehat{\mu}$ increases. The effective viscosity of the porous layer makes the system stable, hence the onset of DBMC is postponed.

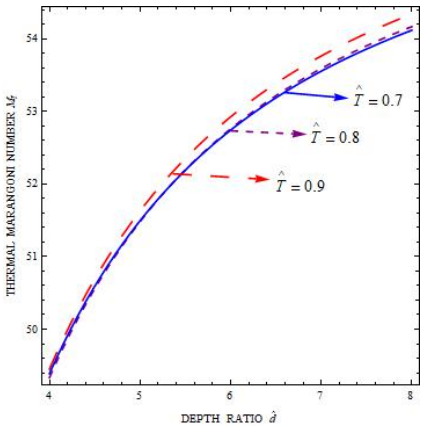

(a)

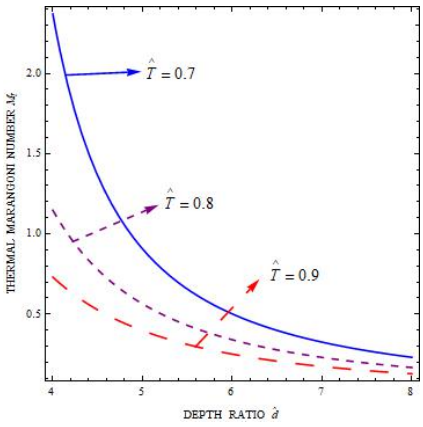

(b)

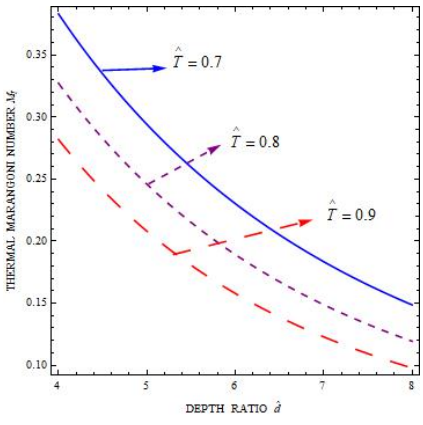

(c)

Figure7: Effects of thermal ratio'$\widehat{T}$'

The effects of the thermal ratio $'\widehat{T}'$ on the thermal Marangoni number are shown in figure 7a, 7b and 7c for linear, parabolic and inverted parabolic profiles respectively for $\widehat{T}$ = 0.7, 0.8 and 0.9. It is seen from the graph that the curves are diverging for linear profile, converging for parabolic profile and the variation effect of $\widehat{T}$ is not altered with all the values of depth ratios for inverted parabolic profile and increase in this parameter increases thermal Marangoni number for linear profile wherein it decreases the same in the other two profiles. So, the increase in the value of thermal ratio makes the system stable hence DBMC is postponed in linear profile and the same is preponed for parabolic and inverted parabolic profiles.

6. Conclusion

The following are the findings from the theoretical investigation of DBMC in a composite layer comprising of couple stress fluid for linear, parabolic and inverted parabolic heat profiles.

i. Increasing values of porous parameter, viscosity ratio and decreasing values of horizontal wavenumber support the stability of DBMC in the presence of all the profiles.

ii. Larger values of couple stress parameters in both the fluid and porous layers and larger values of thermal ratio stabilize DBMC when the composite layer is subjected to linear heat profile.

iii. Lower the values of couple stress parameters and thermal ratio stabilize DBMC when the composite layer is subjected to inverted parabolic heat profile.

iv. The linear heat profile is suitable to control DBMC and the inverted parabolic heat profile to enhance DBMC in a composite layer comprising of couple stress fluid.

References

[1] Anum Shafiq, Islam Zari, Ilyas Khan, Taheer Saeed Khan, Asiful H. Seikh and El-Sayed M. Sherif,Marangoni Driven Boundary Layer Flow of Carbon Nanotubes Toward a Riga Plate, *Frontiers in Physics*, 2020, doi: 10.3389/fphy.2019.00215

[2] Asifa Tassaddiq, Ibni Amin, Meshal Shutaywi, Zahir Shah, Farhad Ali, Saeed Islam and Asad Ullah, Thin Film Flow of Couple Stress Magneto-Hydrodynamics Nanofluid with Convective Heat over an Inclined Exponentially Rotating Stretched Surface, *MDPI, Coatings,* 10(338)(2020).

[3] Giovanni Fantuzzi, Anton Pershin and Andrew Wynn, Bounds on heat transfer for Benard-Marangoni convection at infinite Prandtl number, *J. Fluid Mech.* 837(2018), 562–596.

[4] Gireesha B.J and Sindhu S, MHD natural convection flow of Casson fluid in an annular micro channel containing porous medium with heat generation/absorption, DE GRUYTER, *Nonlinear Engineering,* 9(2020), 223–232.

[5] Gupta A.K and Kalta S.K, Effect of Non-uniform Temperature gradient on Marangoni Convection in a Relatively Hotter or Cooler Layer of Liquid, *Research J. Engineering and Tech.* 6(1)(2015).

[6] Ilani S. S & Ashmawy E. A, A time dependent slip flow of a couple stress fluid between two parallel plates through state space, *Journal of Taibah University for Science,* 12(5)(2018), 592-599.

[7] Mahmud M. N, Idris R and Hashim I, Effects of Magnetic Field and Nonlinear Temperature Profile on Marangoni Convection in Micropolar Fluid, Hindawi Publishing Corporation, *Differential Equations and Nonlinear Mechanics*, 2009, Article ID 748794.

[8] Narasimha Murthy S, Mixed convection of couple stress fluid in a vertical channel in the presence of heat generation or heat absorption, *Ethiop. J. Sci. & Technol,* 7(1)(2014), 49-66.

[9] Nur Zarifah Abdul Hamid, Nor Fadzillah Mohd Mokhtar, Norihan Md Arifin, and Mohammad Hasan Abdul Sathar, Effect of Nonlinear Temperature Profile and Magnetic Field on Thermal Convection in a Binary Fluid Saturated an Anisotropic Porous Medium, *ASM Sc. J.*, 12(1)(2019), 126-136.

[10] Rahmat Ellahi , Ahmed Zeeshan, Farooq Hussain and Tehseen Abbas, Two-Phase Couette Flow of Couple Stress Fluid with Temperature Dependent Viscosity Thermally Affected by Magnetized Moving Surface, MDPI, *Symmetry*, 11(647)(2019), doi:10.3390/sym11050647.

[11] Sameena Tarannum and Pranesh S, Effect of Gravity Modulation on the Onset of Rayleigh-Bénard Convection in a Weak Electrically Conducting Couple Stress Fluid with Saturated Porous Layer, *International Journal of Engineering Research & Technology (IJERT)*, 5(01)(2016).

[12] Sanatan Das, Akram Ali and Rabindra Nath Jana, Slip flow of an optically thin radiating non-gray couple stress fluid past a stretching sheet, *Journal of Heat and Mass Transfer Research,* 1(2016), 21-30.

[13] Shivakumara I.S, Sureshkumar S and Devaraju N, Effect of Non-Uniform Temperature Gradients on the Onset of Convection in a Couple-Stress Fluid-Saturated Porous Medium, *Journal of Applied Fluid Mechanics,* 5(1)(2012), 49-55.

[14] Siti Suzilliana Putri Mohamed Isa, Norihan Md. Arifin, Roslinda Mohd Nazar and Mohd Noor Saad, Combined Effect of Non-Uniform Temperature Gradient and Magnetic Field on Benard-Marangoni Convection with a Constant Heat Flux, *The Open Aerospace Engineering Journal*, 3(2010), 59-64.

[15] Sumithra R, Vanishree R.K and Manjunatha N, Effect of constant heat source / sink on single component Marangoni convection in a composite layer bounded by adiabatic boundaries in presence of uniform & non uniform temperature gradients, *Malaya Journal of Matematik*, 8(2)(2020), 306-313.

[16] Sumithra R and Shyamala Venkatraman, Darcy-Benard Marangoni Convection in a Composite Layer Comprising of Couple Stress Fluid, *International Journal of Applied Engineering Research,* 15(7)(2020), 659-671.

★★★★★★★★★
ISSN(P):2319 – 3786
Malaya Journal of Matematik
ISSN(O):2321 – 5666
★★★★★★★★★